Cytotoxic Ribonucleases: The Dichotomy of Coulombic Forces†

R. Jeremy Johnson,‡ Tzu-Yuan Chao,‡ Luke D. Lavis,§ and Ronald T. Raines*,‡,§

Departments of Biochemistry and Chemistry, University of Wisconsin−Madison, Madison, Wisconsin 53706

Received May 5, 2007; Revised Manuscript Received June 18, 2007

ABSTRACT: Cells tightly regulate their contents. Still, nonspecific Coulombic interactions between cationic molecules and anionic membrane components can lead to adventitious endocytosis. Here, we characterize this process in a natural system. To do so, we create variants of human pancreatic ribonuclease (RNase 1) that differ in net molecular charge. By conjugating a small-molecule latent fluorophore to these variants and using flow cytometry, we are able to determine the kinetic mechanism for RNase 1 internalization into live human cells. We find that internalization increases with solution concentration and is not saturable. Internalization also increases with time to a steady-state level, which varies linearly with molecular charge. In contrast, the rate constant for internalization ($t_{1/2}$ = 2 h) is independent of charge. We conclude that internalization involves an extracellular equilibrium complex between the cationic proteins and abundant anionic cell-surface molecules, followed by rate-limiting internalization. The enhanced internalization of more cationic variants of RNase 1 is, however, countered by their increased affinity for the cytosolic ribonuclease inhibitor protein, which is anionic. Thus, Coulombic forces mediate extracellular and intracellular equilibria in a dichotomous manner that both endangers cells and defends them from the potentially lethal enzymatic activity of ribonucleases.

Cells control their intracellular environment through careful gating of the influx of extracellular material (*1*, *2*). To distinguish between molecules to be internalized and those to be excluded, cells use specific interactions with cell-surface proteins, lipids, and carbohydrates. Nonspecific interactions mediated by Coulombic forces can also lead to internalization, often in an unregulated manner (*1*−*5*).[1] Such nonspecific interactions can be modulated by increasing, decreasing, or masking the cationic charge on the biomolecule (*3*, *5*).

Two classes of molecules that exploit high cationicity to effect nonspecific adsorption to the cell surface and internalization are cell-penetrating peptides (CPPs[2]) and ribonucleases (*7*−*10*). CPPs have received considerable attention because of their ability to transport otherwise membrane-impermeable cargo into cells (*9*, *11*, *12*). The detailed mechanism of CPP internalization is unclear but is known to involve multiple steps. Those steps include binding to anionic cell-surface molecules, internalization in an ATP- and temperature-dependent manner, and ultimately translocation from endosomes into the cytoplasm (*9*, *13*−*15*). Similar to cationic peptides, the endocytosis of pancreatic-type ribonucleases is facilitated by their cationic nature (*10*, *16*). Ribonucleases bind to the cell surface through Coulombic interactions between positively charged residues and negatively charged cell-surface molecules (*10*) and are endocytosed by a dynamin-independent pathway without the necessity for a specific receptor (*16*).

Pancreatic-type ribonucleases have diverse biological activities, including selective toxicity to cancerous cells (*17*−*22*). The archetype of a cytotoxic ribonuclease is Onconase (ONC), a ribonuclease isolated from the oocytes of *Rana pipiens* that is currently in confirmatory phase IIIb clinical trials for the treatment of malignant mesothelioma (*23*). The specific toxicity of ONC and engineered ribonucleases toward tumor cells relies on multiple biochemical attributes, such as evasion of the cytosolic ribonuclease inhibitor protein (RI (*24*)), high ribonucleolytic activity, and resistance to proteolysis (*25*−*27*).

Cationic charge is also important for ribonuclease cytotoxicity. For example, the cytotoxicity of bovine pancreatic ribonuclease (RNase A, EC 3.1.27.5 (*28*)) and microbial ribonucleases can be increased through mutagenic or chemical cationization (*29*−*33*). Traditional studies on the relationship between the cationicity and cytotoxicity of ribonucleases

† This work was supported by Grant CA73808 (NIH). R.J.J. and L.D.L. were supported by Biotechnology Training Grant 08349 (NIH). L.D.L. was also supported by an ACS Division of Organic Chemistry Fellowship, sponsored by the Genentech Foundation. The Biophysics Instrumentation Facility was established with Grants BIR-9512577 (NSF) and RR13790 (NIH).

* To whom correspondence should be addressed. Department of Biochemistry, University of Wisconsin−Madison, 433 Babcock Drive, Madison, WI 53706-1544. Tel: 608-262-8588. Fax: 608-262-3453. E-mail: raines@biochem.wisc.edu.

‡ Department of Biochemistry.

§ Department of Chemistry.

[1] We prefer to use the term *Coulombic* rather than *electrostatic* to describe the force between two point charges. We consider electrostatic to be a general term that encompasses Coulombic forces, hydrogen bonds, and dipole−dipole interactions. Coulombic is thus a more specific term, referring only to interactions that obey Coulomb's law: $F = q_1q_2/(4\pi\epsilon r^2)$ (*6*).

[2] Abbreviations: CPP, cell-penetrating peptide; DTT, dithiothreitol; 6-FAM, 6-carboxyfluorescein; MALDI−TOF, matrix-assisted laser desorption/ionization−time-of-flight; ONC, Onconase (a registered trademark of Alfacell, Inc.); PBS, phosphate-buffered saline; PDB, Protein Data Bank; RI, ribonuclease inhibitor; RNase A, bovine pancreatic ribonuclease; RNase 1, human pancreatic ribonuclease; 6-TAMRA, 6-carboxytetramethylrhodamine; *Z*, net molecular charge: Arg + Lys − Asp − Glu.

10.1021/bi700857u CCC: $37.00
Published on Web 08/18/2007

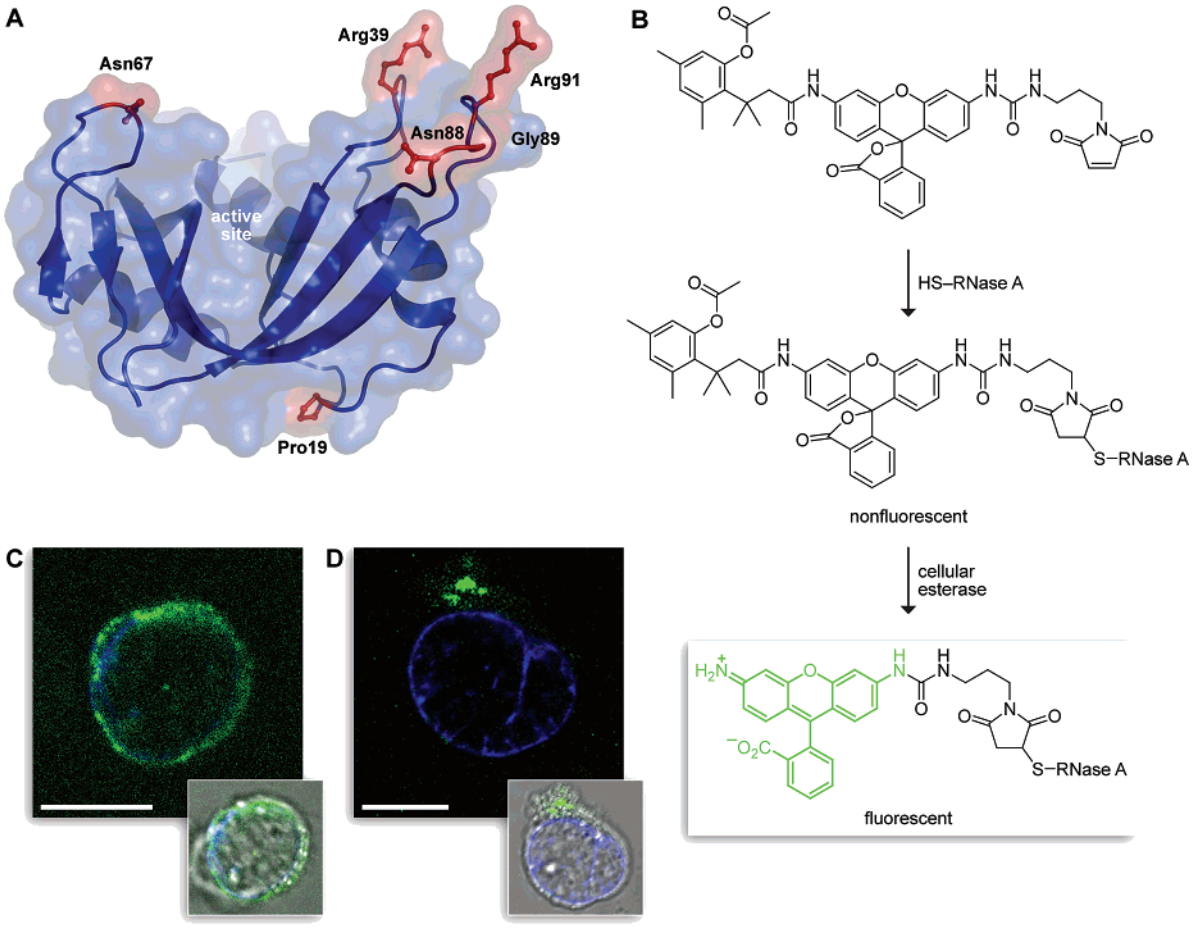

FIGURE 1: Design of ribonuclease variants and latent fluorophore. (A) Ribbon diagram of RNase 1 (PDB entry 1Z7X, chain Z (*40*)). Residues substituted herein are depicted in red. The image was created with the program PyMOL (DeLano Scientific, South San Francisco, CA). (B) Structure of latent fluorophore before and after activation by an intracellular esterase. (C and D) Confocal microscopy images of unwashed K-562 cells incubated at 37 °C for 30 min with fluorescein-labeled RNase 1 (10 μM; C) or latent fluorophore-labeled RNase 1 (10 μM; D). Nuclei were stained by adding Hoechst 33342 (2 μg/mL) during the final 5 min of incubation. Insets: bright-field images. Scale bar: 10 μm.

have used cell death as the read-out (*10*, *29*−*34*). This phenotype is manifested, however, only after a complex, multistep process (*17*−*22*). Hence, a direct measurement of ribonuclease internalization is necessary to dissect the effect of cationicity on internalization.

Here, we isolate internalization from cell death by using a novel fluorogenic label with fluorescence that remains quiescent until an encounter with an intracellular esterase (*35*, *36*). By using this latent fluorophore along with flow cytometry, we directly quantitate the internalization of variants of human pancreatic ribonuclease (RNase 1; Figure 1A). We then characterize the effect of charge on two equilibria that mediate ribonuclease cytotoxicity. Our findings reveal new information about the role of Coulombic forces in protein−cell and protein−protein interactions.

EXPERIMENTAL PROCEDURES

Materials. *Escherichia coli* strain BL21(DE3) was from Novagen (Madison, WI). 6-FAM−dArU(dA)$_2$−6-TAMRA, a fluorogenic ribonuclease substrate, was from Integrated DNA Technologies (Coralville, IA). Enzymes were from Promega (Madison, WI). K-562 cells, which are an erythroleukemia cell line derived from a chronic myeloid leukemia patient, were from the American Type Culture Collection (Manassas, VA). Cell culture medium and supplements were from Invitrogen (Carlsbad, CA). [*methyl*-^{3}H]Thymidine (6.7 Ci/mmol) was from Perkin−Elmer (Boston, MA). Protein purification columns were from GE Biosciences (Piscataway, NJ). MES buffer (Sigma−Aldrich, St. Louis, MO) was purified by anion-exchange chromatography to remove trace amounts of oligomeric vinylsulfonic acid (*37*). Phosphate-buffered saline (PBS) contained (in 1.00 L) NaCl (8.0 g), KCl (2.0 g), $Na_2HPO_4{\cdot}7H_2O$ (1.15 g), KH_2PO_4 (2.0 g), and NaN_3 (0.10 g) and had a pH of 7.4. All other chemicals were of commercial grade or better and were used without further purification.

Instrumentation. Fluorescence spectroscopy was performed with a QuantaMaster1 photon-counting fluorimeter equipped with sample stirring (Photon Technology International, South Brunswick, NJ). Thermal denaturation data were collected using a Cary 3 double-beam spectrophotometer equipped with a Cary temperature controller (Varian, Palo Alto, CA). [*methyl*-^{3}H]Thymidine incorporation into genomic DNA was quantitated by liquid scintillation counting using a Microbeta TriLux liquid scintillation and luminescence counter (Perkin−Elmer, Wellesley, MA). The mass of RNase 1 and its variants was confirmed by matrix-assisted laser desorption/ionization time-of-flight (MALDI−TOF) mass spectrometry with a Voyager-DE-PRO Biospectrometry Workstation (Applied Biosystems, Foster City, CA) at the campus Biophysics

Instrumentation Facility. Flow cytometry data were collected by using a FACSCalibur flow cytometer equipped with a 488-nm argon-ion laser (Becton Dickinson, Franklin Lakes, NJ). Microscopy images were obtained with a Nikon Eclipse TE2000-U confocal microscope equipped with a Zeiss AxioCam digital camera.

Protein Purification and Labeling. DNA encoding variants of RNase 1 were made by using plasmid pHP-RNase (*38*) and the Quikchange site-directed mutagenesis or Quikchange Multi site-directed mutagenesis kit (Stratagene, La Jolla, CA). RNase 1 variants were produced in *E. coli* and purified by using methods described previously for wild-type RNase 1 (*38*). D38R/R39D/N67R/G88R RNase A, which is a highly cytotoxic variant (*39*), was a gift from T. J. Rutkoski. Human RI was produced in *E. coli* and purified as described previously (*40*).

Variants with a free cysteine at position 19 were protected by reaction with 5,5′-dithio-bis(2-nitrobenzoic acid) (DTNB) (*36*, *41*). Immediately prior to latent-fluorophore attachment, TNB-protected ribonucleases were deprotected with a 3-fold molar excess of dithiothreitol (DTT) and desalted by chromatography on a PD-10 desalting column (GE Biosciences, Piscataway, NJ). The maleimide-containing latent fluorophore was synthesized as described previously (*36*). Deprotected ribonucleases were reacted for 4−6 h at 25 °C with a 10-fold molar excess of thiol-reactive latent fluorophore (*36*). Conjugates were purified by chromatography using a HiTrap SP FF column. The molecular masses of RNase 1, its variants, and conjugates were confirmed by MALDI−TOF mass spectrometry. Protein concentration was determined by using a bicinchoninic acid assay kit from Pierce (Rockford, IL) with bovine serum albumin as a standard.

Conformational Stability Measurements. The conformational stability of RNase 1 and its variants was determined by following the change in UV absorbance at 287 nm with increasing temperature (*26*). The temperature of PBS containing an RNase 1 variant (0.1−0.2 mg/mL) was heated from 20 to 80 °C at 0.15 °C/min. The A_{287} was followed at 1 °C intervals, and the absorbance change was fitted to a two-state model of denaturation, wherein the temperature at the midpoint of the transition curve corresponds to the value of T_m.

Ribonucleolytic Activity Assays. The ribonucleolytic activity of RNase 1 and its variants was determined by quantitating its ability to cleave 6-FAM−dArU(dA)$_2$−6-TAMRA (*42*). Assays were carried out at 23 (±2) °C in 2.0 mL of 0.10 M MES−NaOH buffer (pH 6.0) containing NaCl (0.10 M). Fluorescence data were fitted to eq 1, in which $\Delta I/\Delta t$ is the initial reaction velocity, I_0 is the fluorescence intensity before addition of a ribonuclease, I_f is the fluorescence intensity after complete substrate hydrolysis, and [E] is the total ribonuclease concentration.

$$k_{cat}/K_M = \frac{(\Delta I/\Delta t)}{(I_f - I_0)[E]} \quad (1)$$

RI-Binding Assays. The affinity of RNase 1 variants for human RI was determined by using a fluorescent competition assay reported previously (*43*). Briefly, PBS (2.0 mL) containing DTT (5 mM), fluorescein-labeled G88R RNase A (50 nM), and various concentrations of an unlabeled RNase 1 variant was incubated at 23 (±2) °C for 20 min. The initial fluorescence intensity of the unbound fluorescein-labeled G88R RNase A was monitored for 3 min (excitation: 491 nm, emission: 511 nm). RI (50 nM) was then added, and the final fluorescence intensity was measured. The value of K_d for RI·RNase 1 complexes as defined in eq 2 was obtained by nonlinear least-squares analysis of the binding isotherm using GraphPad Prism 4.02 (GraphPad Software, San Diego, CA). The K_d value for the complex between RI and fluorescein-labeled G88R RNase A was taken to be 1.4 nM (*39*).

$$\text{RI·RNase 1} \overset{K_d}{\rightleftharpoons} \text{RI} + \text{RNase 1} \quad (2)$$

Cytotoxicity Assays. The effect of RNase 1 and its variants on the proliferation of K-562 cells was assayed as described previously (*38*, *39*, *44*). After a 44-h incubation with ribonuclease, K-562 cells were treated with [*methyl*-^{3}H]-thymidine for 4 h, and the incorporation of radioactive thymidine into cellular DNA was quantitated by liquid scintillation counting. The results are shown as the percentage of [*methyl*-^{3}H]thymidine incorporated relative to control cells. Data are the average of three measurements for each concentration, and the entire experiment was repeated in triplicate. Values for IC_{50} were calculated by fitting the curves by nonlinear regression with eq 3 (*39*), in which y is the total DNA synthesis following the [*methyl*-^{3}H]thymidine pulse, and h is the slope of the curve.

$$y = \frac{100\%}{1 + 10^{(\log(IC_{50}) - \log[\text{ribonuclease}])h}} \quad (3)$$

Flow Cytometry Assays. The internalization of ribonuclease variants with latent fluorophore attached (Figure 1B) was followed by monitoring the unmasking of fluorescence by intracellular esterases. K-562 cells from near confluent flasks were collected by centrifugation and resuspended at a density of 1×10^6 cells/mL in fresh RPMI 1640. Labeled ribonuclease (10 μM) or unlabeled RNase 1 (10 μM) was added to 250 μL of RPMI containing 1×10^6 cells/mL of K-562 cells. K-562 cells were allowed to incubate at 37 °C for varying times with the ribonucleases. To quench internalization, K-562 cells were collected by centrifugation at 750*g* for 3 min at 4 °C, and cell pellets were resuspended gently in ice-cold PBS (250 μL). Samples remained on ice until analyzed by flow cytometry.

Latent fluorophore fluorescence was detected through a 530/30-nm band-pass filter. Cell viability was determined by staining with propidium iodide, which was detected through a 660-nm long-pass filter. The mean channel fluorescence intensity of 20,000 viable cells was determined for each sample using CellQuest software and used for subsequent analysis. To determine the steady-state rate constant for ribonuclease internalization, fluorescence intensity data were fitted to eq 4, in which F_{max} is the fluorescence intensity upon reaching the steady state, and k_I is the rate constant for ribonuclease internalization into K-562 cells.

$$F = F_{max}(1 - e^{-k_I t}) \quad (4)$$

Microscopy. Confocal microscopy was used to observe ribonuclease localization. K-562 cells were prepared as

Table 1: Properties of Wild-Type RNase 1 and its Variants

RNase 1	T_m (°C)[a]	k_{cat}/K_M (10^6 $M^{-1}s^{-1}$)[b]	K_d (nM)[c]	IC_{50} (μM)[d]	Z
wild type[e]	57	21 ± 2	29×10^{-8}	>25	+6
DDADD[e]	58	6.3 ± 0.5	(1.7 ± 0.5) × 10^3	13.3 ± 1.7	0
LLALL[e]	65	30 ± 3	30 ± 1	>25	+4
DRRDD	53	14 ± 3	28 ± 4	5.69 ± 0.37	+3
DRRRD	49	6.7 ± 0.6	1.3 ± 0.2	10.8 ± 0.93	+5
LRRDD	54	19 ± 2	1.8 ± 0.1	16.2 ± 1.3	+4
LRRRD	53	9.1 ± 2	1.1 ± 0.2	>25	+6

[a] Values of T_m (±2 °C) were determined in PBS by UV spectroscopy. [b] Values of k_{cat}/K_M (±SE) were determined for the catalysis of 6-FAM−dArU(dA)$_2$−6-TAMRA cleavage at 25 °C in 0.10 M MES−NaOH buffer (OVS-free) at pH 6.0, containing 0.10 M NaCl and were calculated with eq 1. [c] Values of K_d (±SE) were determined for the complex with human RI (eq 2) at 25 °C. [d] Values of IC_{50} (±SE) are for incorporation of [*methyl*-^{3}H]thymidine into the DNA of K-562 cells treated with the ribonuclease and were calculated with eq 3. [e] From ref *40*.

described for flow cytometry. Latent fluorophore-labeled RNase 1 variant (10 μM) or fluorescein-labeled RNase 1 variant (10 μM) were added to 250 μL of RPMI 1640 containing K-562 cells (1×10^6 cells/mL) and incubated at 37 °C for varying times. Cell nuclei were stained by the addition of Hoechst 33342 (2 μg/mL) for the final 5 min of incubation. Excitation at 408 nm was provided by a blue-diode laser, and emission light was passed through a filter centered at 450 nm with a 35-nm band-pass. Excitation at 488 nm was provided by an argon-ion laser, and emission light was passed through a filter centered at 515 nm with a 40-nm band-pass. Excitation at 543 nm was provided by a HeNe laser, and emission light was passed through a filter centered at 605 nm with a 75-nm band-pass.

RESULTS

Design of RNase 1 Variants. Recently, we reported on variants of RNase 1 that evade the inhibitory action of RI (*40*). In these variants, positions 39, 67, 88, 89, and 91 of RNase 1 were determined to be important contact residues between human RI and RNase 1 (Figure 1A). By engendering Coulombic repulsion at these positions, a variant of RNase 1 (DDADD[3]) was endowed with 5×10^9-fold lower affinity for RI. This variant was, however, only moderately toxic to human chronic myeloid leukemia cells *in vitro* (IC_{50} = 13.3 μM) (*40*).

The lowered cytotoxicity of this RNase 1 variant when compared to other ribonucleases with similar biochemical characteristics was proposed to result from its net neutral charge, which could diminish its cellular internalization (*40*). To investigate the effect of both positively and negatively charged amino acid substitutions at these same positions in RNase 1 on ribonuclease internalization and RI evasion, a series of RNase 1 variants were constructed (Table 1). To maintain a basal level of RI evasion and cytotoxicity, these RNase 1 variants maintained an aspartate or leucine substitution at positions 39 and 91, as these residues contributed most to the evasion of RI (*40*). Then, the net charge of the RNase 1 variant was varied by incorporating positively or negatively charged residues at positions 67, 88, or 89, which are known to contribute less to the stability of the RI·RNase 1 complex (*40*). These substitutions neither create nor destroy a canonical nuclear localization signal, which could contribute to cytotoxicity (*45*). The resulting RNase 1 variants had a net charge (Z) ranging from 0 to +6.

[3] RNase 1 variants are named according to their amino acid composition at residues 39, 67, 88, 89, and 91. Hence, DDADD RNase 1 refers to the R39D/N67D/N88A/G89D/R91D variant.

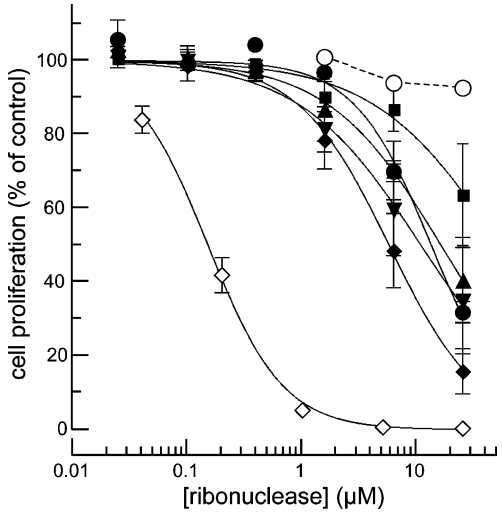

FIGURE 2: Cytotoxicity of ribonuclease variants. Effect of ribonucleases on the proliferation of K-562 cells was determined by monitoring the incorporation of [*methyl*-^{3}H]thymidine into cellular DNA in the presence of ribonucleases. Data points are mean values (±SE) from ≥3 experiments, each carried out in triplicate, and were fitted to eq 3. Variants in order of increasing cytotoxicity: D38R/R39D/N67R/G88R RNase A (◇); DRRDD RNase 1 (♦); DRRRD RNase 1 (▼); DDADD RNase 1 (●); LRRDD RNase 1 (▲); LRRRD RNase 1 (■); and wild-type RNase 1 (○).

Biochemical Properties of RNase 1 Variants. The cytotoxicity of a ribonuclease is governed by the biochemical parameters listed in Table 1 (*25*−*27*): conformational stability, ribonucleolytic activity, RI affinity, and molecular charge of the RNase 1 variants. The conformational stability of a ribonuclease, which provides a measure of its vulnerability to proteolysis, correlates with its cytotoxic activity (*26*). Conformational stability could not, however, have had a significant effect on the cytotoxicity of the RNase 1 variants, as each T_m value is within 8 °C of that of wild-type RNase 1 and significantly above physiological temperature (37 °C). Like conformational stability, ribonucleolytic activity correlates with cytotoxicity (*25*, *46*). Here, however, each of the RNase 1 variants cleaved an RNA substrate with a k_{cat}/K_M value that was within 3-fold of that of the wild-type enzyme (*42*).

The biochemical attribute that varied most dramatically between the different RNase 1 variants was the affinity for RI (Table 1), which is known to be an important factor in cytotoxicity (*25*, *39*, *44*, *47*). Consequently, the 1500-fold range of affinities for RI, between the most RI-evasive variant (DDADD RNase 1; K_d = 1.7 μM) and the least RI-evasive variant (LRRRD RNase 1; K_d = 1.1 nM), foreshadows a large range of cytotoxic activity.

Ribonuclease Cytotoxicity. Surprisingly, the RNase 1 variants varied little in their cytotoxic activity (Figure 2; Table 1). None of the RNase 1 variants was as cytotoxic as D38R/R39D/N67R/G88R RNase A. This variant of the bovine enzyme is both highly evasive of RI (K_d = 510 nM) and highly cationic, having a net molecular charge (i.e., Arg + Lys − Asp − Glu) of Z = +6 (*39*).

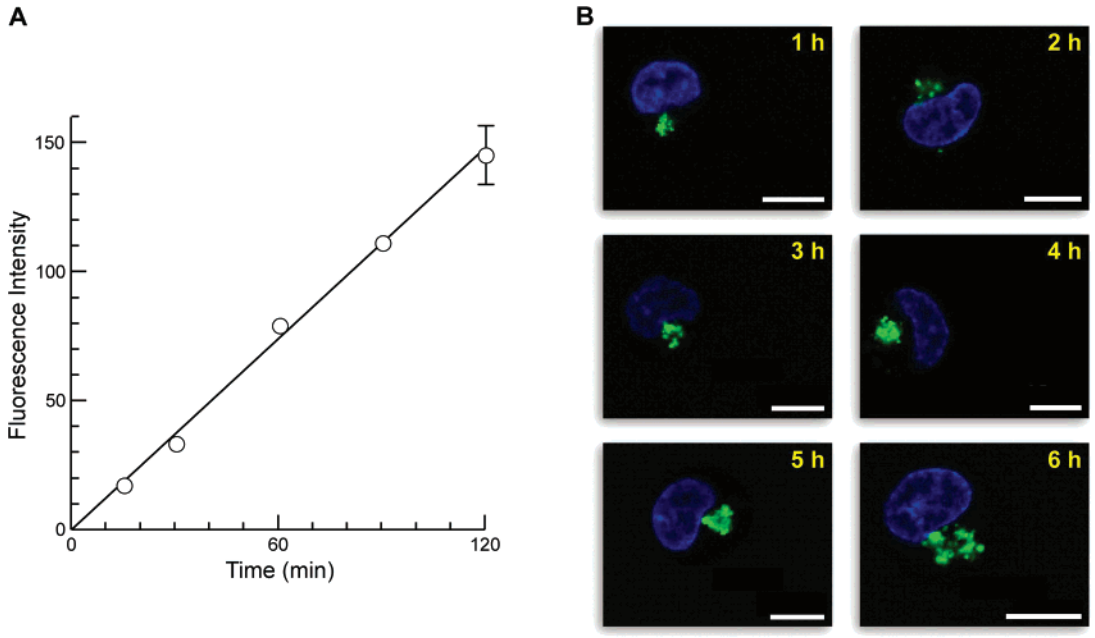

FIGURE 3: Kinetics of ribonuclease internalization. (A) Initial velocity of cellular internalization vs time (≤2 h). Internalization was determined by incubating latent fluorophore-labeled RNase 1 (○) with K-562 cells at 37 °C. Incubations were quenched at known times by immersing the K-562 cells in ice-cold PBS and storing them on ice before quantitation by flow cytometry. Data points are mean values (±SE) from ≥3 cell populations. (B) Confocal microscopy images of unwashed K-562 cells incubated at 37 °C for varying time periods (0−6 h) with latent fluorophore-labeled RNase 1 (10 μM). Nuclei were stained by adding Hoechst 33342 (2 μg/mL) during the final 5 min of incubation. Scale bar: 10 μm.

Ribonuclease Internalization. To determine whether the molecular charge of an RNase 1 variant affects its cellular internalization, we employed a synthetic latent fluorophore (Figure 1B) (*35*, *36*). This latent fluorophore is not fluorescent until activated by an intracellular esterase, allowing for the direct and continuous visualization of protein internalization (Figure 1C and D). RNase 1, like RNase A, has eight cysteine residues that form four disulfide bonds in the native enzyme. To enable the attachment of the latent fluorophore, we replaced Pro19 of each RNase 1 variant with a cysteine residue. Position 19 was chosen because it is remote from the regions of interest (Figure 1A), and attachment of fluorescent groups at this position is not known to have a detectable effect on the ribonucleolytic activity, RI-affinity, or cell-surface binding of ribonuclease variants (*16*, *43*). The latent fluorophore was attached to Cys19 of each ribonuclease by a standard maleimide coupling reaction (*36*).

The internalization of latent fluorophore-conjugated ribonuclease variants was observed by fluorescence microscopy and quantitated by flow cytometry. Initial experiments revealed that the amount of ribonuclease internalized into live human cells increased linearly during the first 2 h (Figure 3A) and accumulated in endocytic vesicles (Figure 3B). Bright-field images indicated that the cells were alive and appeared to have normal physiology during the time course of the experiments (Figure 1D).

Detailed experiments were then performed to quantify the internalization of a ribonuclease as a function of time (Figure 4A), its net charge (Figure 4B), and its concentration (Figure 4C). Using eq 4 and the data in Figure 4A, the values of $t_{1/2}$ (= ln 2/k_i) for the internalization of the RNase 1 variants were calculated to be (110 ± 17) min for RNase 1, (131 ± 16) min for DRRDD RNase 1, and (129 ± 26) min for DDADD RNase 1. These $t_{1/2}$ values are indistinguishable, suggesting that each variant is endocytosed by the same mechanism.

The amount of ribonuclease internalized into K-562 cells in 30 min was related linearly to the net charge of the ribonuclease (Figure 4B). The relative amount of ribonuclease internalized at 30 min also increased by greater than 4-fold between the RNase 1 variants with the lowest and highest net charge (DDADD (Z = 0) and LRRRD (Z = +6), respectively). Two variants of RNase 1 (DRRRD and LRRRD, with the G89R substitution underlined) were internalized to a somewhat greater extent than expected based on their net charge. These two variants are the only ones with a G89R substitution.

The amount of ribonuclease internalized into K-562 cells in 30 min increased with the solution concentration of the ribonuclease, at least up to 10 μM (Figure 4C). These data suggest that the binding of RNase 1 to the cell surface is not saturable (*16*), consistent with internalization being mediated by a nonspecific interaction with an abundant cell-surface molecule rather than by a specific interaction with a receptor. Again, internalization correlated with net charge, as more wild-type RNase 1 (Z = +6) than its DRRDD (Z = +3) or DDADD (Z = 0) variant was internalized at each concentration.

DISCUSSION

Dual Influence of Coulombic Forces. Coulombic forces can lead to the unregulated internalization of cationic peptides and proteins into cells (*1*−*5*). To assess the biological consequences of increasing the charge of a ribonuclease, we created RNase 1 variants with a range of net charges (Table 1). We then quantitated their cellular internalization by using a latent fluorophore (Figure 1B) and flow cytometry. This

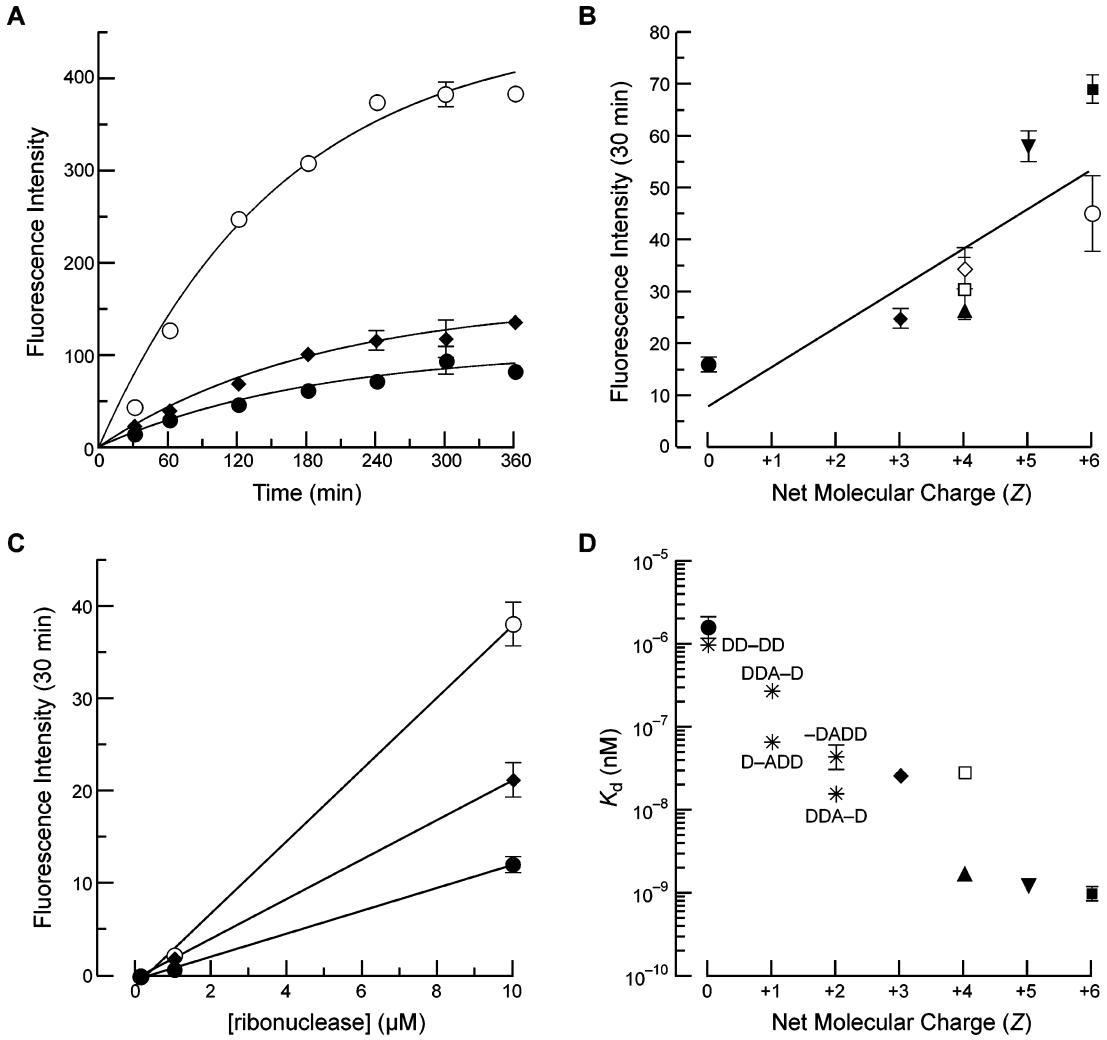

FIGURE 4: Properties of RNase 1, its variants, and RNase A: wild-type RNase 1 (○), DDADD RNase 1 (●), DRRDD RNase 1 (♦), LRRDD RNase 1 (▲), LLALL RNase 1 (□), DRRRD RNase 1 (▼), LRRRD RNase 1 (■), and wild-type RNase A (◊). (A) Plot of internalization of a ribonuclease into K-562 cells vs time. Internalization was measured by using flow cytometry and following the fluorescence manifested by activation of a latent fluorophore attached to the ribonuclease (10 μM) after incubation for the specified times points. Data points are the mean values (±SE) for 20,000 cells from ≥3 cell populations and were fitted to eq 4. (B) Plot of internalization of a ribonuclease into K-562 cells vs its net charge. Internalization was monitored as in panel A, except that all incubations were for 30 min at 37 °C. (C) Plot of internalization of a ribonuclease into K-562 cells vs its concentration. Internalization was followed as in panel A, except for the variable concentration of ribonuclease (0.1, 1.0, or 10 μM). (D) Semilog plot of affinity of a ribonuclease for RI vs its net charge. Data points are the mean values (±SE). Variants of RNase 1 from ref *40* are indicated by an asterisk and their amino acids at positions 39, 67, 88, 89, and 91, with "−" indicating the wild-type residue.

combination obviated any signal from ribonucleases bound to the cell membrane (Figure 1C) without the need for protease treatment or washing steps (*15*, *36*), permitting more timely and precise measurements than are accessible with any other method.

The net charge of a ribonuclease has a positive linear relationship with its internalization (Figure 4B). The two variants with the highest internalization based on their net charge have an arginine residue at position 89 (DRRRD and LRRRD). Installing arginine in the analogous site of RNase A yielded G88R RNase A, which was the first monomeric mammalian ribonuclease endowed with cytotoxicity (*47*). This cytotoxicity was attributed to a 10^4-fold decrease in affinity for RI (*47*). Our analyses of the G89R variants of RNase 1 suggest, however, that this substitution in RNase A could instill the added benefit of increasing cellular internalization. Our data also indicate that a positive net charge is *not* essential for ribonuclease internalization, as a neutral RNase 1 variant (DDADD) is internalized significantly and is cytotoxic (Figures 2 and 4; Table 1). Instead, the disposition of charge could govern the internalization of ribonucleases (*10*) and other proteins (*48*).

The opposite trend is observed between charge and the affinity for RI, which is highly anionic ($Z = -22$). In Figure 4D, the net charge of RNase 1 variants substituted at positions 39, 67, 88, 89, and 91 is plotted versus the K_d value for their complex with RI. An inverse relationship between the net charge of an RNase 1 variant and its affinity for RI is observed, reinforcing the unusual nature of the RI−RNase 1 interaction and the importance of Coulombic forces to RI·RNase 1 complex formation (*40*).

Hence, two competing equilibria involving ribonuclease charge seem to imperil and protect cells from the cytotoxic activity of rogue ribonucleases (*16*). In these equilibria, increasing the positive charge of a ribonuclease increases its internalization but also increases its RI affinity (Figure

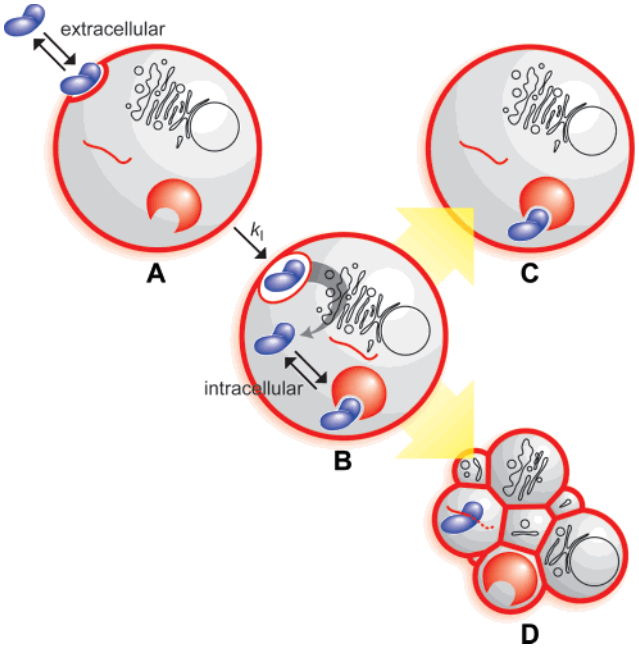

FIGURE 5: Coulombic effects on ribonuclease-mediated cytotoxicity. Cationic and anionic molecules are depicted in blue and red, respectively. (A) Ribonucleases form an extracellular equilibrium complex with abundant anionic cell-surface molecules such as heparan sulfate. Bound ribonucleases are internalized into endosomes with rate constant k_I. (B) Internalized ribonucleases translocate to the cytosol by an unknown mechanism. (C) In the cytosol, ribonucleases form an intracellular equilibrium complex with RI. (D) Ribonucleases that evade RI degrade cellular RNA, leading to apoptosis.

4), yielding RNase 1 variants with similar cytotoxic activity (Figure 2; Table 1). These competing equilibria make net charge a difficult variable to optimize in the design of cytotoxic ribonucleases.

Mechanism of Ribonuclease Internalization. The internalization of a ribonuclease seems to limit its cytotoxicity, as microinjected ribonucleases are cytotoxic at picomolar concentrations (*49*). Thus, fully understanding the factors involved in ribonuclease internalization could lead to more effective ribonuclease chemotherapeutics (*16*). The cationicity of RI-evasive ribonucleases correlates with their cytotoxicity (*29*−*32*) and destabilization of anionic membranes (*10*). The endocytic mechanism is dynamin-independent (*16*), but the remaining steps in the pathway are unknown.

Further insight into the mechanism of ribonuclease internalization can be gathered by comparing its kinetic mechanism to that of CPPs. CPP internalization reaches a steady-state level, like that of ribonucleases (Figure 4A) (*13*, *50*). The half-time for the internalization of a CPP ($t_{1/2} \leq 60$ min (*11*, *13*)) is, however, less than that for the internalization of an RNase 1 variant ($t_{1/2} = 2$ h, Figure 4A). This difference in rate constant likely arises from the difference in molecular mass, as CPPs carrying large cargo internalize more slowly (*11*). As with ribonucleases (Figure 4C), CPP internalization is dose-dependent (*13*). These similarities are consistent with ribonucleases and CPPs having similar internalization mechanisms.

The steady-state kinetics of CPP internalization have been interpreted in terms of an equilibrium formed between CPP free in solution and CPP bound to anionic cell-surface molecules, concomitant with the degradation of the CPP (*11*, *13*, *50*). On the basis of the similarities between CPPs and ribonucleases, the same explanation seems to be applicable for ribonucleases: an extracellular pre-equilibrium is formed between ribonuclease free in solution and bound to the cell surface. Further evidence for the existence of such a prior equilibrium is provided by the charge dependence of internalization. All three ribonucleases tested had a similar half-time for internalization (2 h), indicative of the same mechanism of internalization. Yet, their steady-state level of internalization varied by up to 4-fold on the basis of their net charge (Figure 4A). Thus, ribonucleases that are more cationic have higher affinities for anionic cell-surface molecules, shifting the extracellular distribution toward the cell-surface bound state. This shift in distribution leads to more ribonucleases being internalized in the rate-limiting step (k_I) but without affecting the internalization rate of any individual molecule.

On the basis of these data, we propose a model for the effect of ribonuclease charge on internalization and cytotoxicity (Figure 5). First, ribonucleases form an extracellular equilibrium with an anionic cell-surface molecule that is mediated by the cationicity of the ribonuclease. A candidate for this cell-surface molecule is heparan sulfate, which is an abundant glycosaminoglycan necessary for the efficient internalization of ribonucleases (*51*) and CPPs (*14*) as well as a cationic variant of the green fluorescent protein (*48*). Second, an intracellular equilibrium based on ribonuclease charge is formed upon ribonuclease translocation to the cytosol (Figure 5). This second equilibrium between ribonucleases bound by RI and those that evade RI is apparent by the opposing trends depicted in Figure 4B and D. In these figures, ribonucleases that are internalized at a higher rate (Figure 4B) are not necessarily more cytotoxic (Figure 2) because they are also bound more tightly by RI (Figure 4D).

Finally, the Coulombic interactions characterized herein could have clinical significance. Cells derived from cancerous tissue tend to be more anionic than cells derived from similar normal tissue (*52*, *53*). In contrast, RI levels are constant in cells with a cancerous and noncancerous origin (*54*). Accordingly, variation in the position of the extracellular equilibrium (Figure 5) could contribute to the therapeutic index of ONC and other ribonucleases.

Conclusions. Understanding how cationic proteins enter human cells and exerting control over this process portends the development of better chemotherapeutics. Toward this end, we developed a method to quantitate the effect of the net charge of a ribonuclease on its cellular internalization. We found ribonuclease internalization to be related linearly to net charge and to reach a steady-state level of internalization based on that net charge. These two characteristics suggest that ribonuclease internalization is controlled by an extracellular equilibrium formed between ribonuclease molecules free in solution and those bound to anionic moieties on the cell surface. This extracellular equilibrium is then counteracted by an intracellular equilibrium in which more cationic ribonucleases bind more tightly to RI. Thus, these two equilibria cause cells to entice and then entrap ribonucleases.

ACKNOWLEDGMENT

We are grateful to W. W. Cleland, T. J. Rutkoski, S. M. Fuchs, and R. F. Turcotte for contributive discussions.

REFERENCES

1. Conner, S. D., and Schmid, S. L. (2003) Regulated portals of entry into the cell, *Nature 422*, 37−44.
2. Polo, S., and Di Fiore, P. P. (2006) Endocytosis conducts the cell signaling orchestra, *Cell 124*, 897−900.
3. Murray, D., and Honig, B. (2002) Electrostatic control of the membrane targeting of C2 domains, *Mol. Cell 9*, 145−154.
4. Cho, W., and Stahelin, R. V. (2005) Membrane-protein interactions in cell signaling and membrane trafficking, *Annu. Rev. Biophys. Biomol. Struct. 34*, 119−151.
5. Mulgrew-Nesbitt, A., Diraviyam, K., Wang, J., Singh, S., Murray, P., Li, Z., Rogers, L., Mirkovic, N., and Murray, D. (2006) The role of electrostatics in protein-membrane interactions, *Biochim. Biophys. Acta 1761*, 812−826.
6. Gillmor, C. S. (1971) *Coulomb and the Evolution of Physics and Engineering in Eighteenth-Century France*, Princeton University Press, Princeton, NJ.
7. Fotin-Mleczek, M., Fischer, R., and Brock, R. (2005) Endocytosis and cationic cell-penetrating peptides—a merger of concepts and methods, *Curr. Pharm. Des. 11*, 3613−3628.
8. Kaplan, I. M., Wadia, J. S., and Dowdy, S. F. (2005) Cationic TAT peptide transduction domain enters cells by macropinocytosis, *J. Controlled Release 102*, 247−253.
9. Fuchs, S. M., and Raines, R. T. (2006) Internalization of cationic peptides: The road less (or more?) traveled, *Cell. Mol. Life Sci. 63*, 1819−1822.
10. Notomista, E., Mancheno, J. M., Crescenzi, O., Di Donato, A., Gavilanes, J., and D'Alessio, G. (2006) The role of electrostatic interactions in the antitumor activity of dimeric RNases, *FEBS J. 273*, 3687−3697.
11. Zorko, M., and Langel, U. (2005) Cell-penetrating peptides: Mechanism and kinetics of cargo delivery, *Adv. Drug Delivery Rev. 57*, 529−545.
12. Chauhan, A., Tikoo, A., Kapur, A. K., and Singh, M. (2006) The taming of the cell penetrating domain of the HIV Tat: Myths and realities, *J. Controlled Release 117*, 148−162.
13. Drin, G., Cottin, S., Blanc, E., Rees, A. R., and Temsamani, J. (2003) Studies on the internalization mechanism of cationic cell-penetrating peptides, *J. Biol. Chem. 278*, 31192−31201.
14. Fuchs, S. M., and Raines, R. T. (2004) Pathway for polyarginine entry into mammalian cells, *Biochemistry 43*, 2438−2444.
15. Richard, J. P., Melikov, K., Brooks, H., Prevot, P., Lebleu, B., and Chernomordik, L. V. (2005) Cellular uptake of unconjugated TAT peptide involves clathrin-dependent endocytosis and heparan sulfate receptors, *J. Biol. Chem. 280*, 15300−15306.
16. Haigis, M. C., and Raines, R. T. (2003) Secretory ribonucleases are internalized by a dynamin-independent endocytic pathway, *J. Cell Sci. 116*, 313−324.
17. D'Alessio, G., and Riordan, J. F., Eds. (1997) *Ribonucleases: Structures and Functions*, Academic Press, New York.
18. Leland, P. A., and Raines, R. T. (2001) Cancer chemotherapy—ribonucleases to the rescue. *Chem. Biol. 8*, 405−413.
19. Matoušek, J. (2001) Ribonucleases and their antitumor activity. *Comp. Biochem. Physiol., C 129*, 175−191.
20. Makarov, A. A., and Ilinskaya, O. N. (2003) Cytotoxic ribonucleases: Molecular weapons and their targets, *FEBS Lett. 540*, 15−20.
21. Benito, A., Ribó, M., and Vilanova, M. (2005) On the track of antitumor ribonucleases, *Mol. Biosyst. 1*, 294−302.
22. Arnold, U., and Ulbrich-Hofmann, R. (2006) Natural and engineered ribonucleases as potential cancer therapeutics, *Biotechnol. Lett. 28*, 1615−1622.
23. Pavlakis, N., and Vogelzang, N. J. (2006) Ranpirnase—an antitumour ribonuclease: Its potential role in malignant mesothelioma, *Expert Opin. Biol. Ther. 6*, 391−399.
24. Dickson, K. A., Haigis, M. C., and Raines, R. T. (2005) Ribonuclease inhibitor: structure and function, *Prog. Nucleic Acid Res. Mol. Biol. 80*, 349−374.
25. Bretscher, L. E., Abel, R. L., and Raines, R. T. (2000) A ribonuclease A variant with low catalytic activity but high cytotoxicity, *J. Biol. Chem. 275*, 9893−9896.
26. Klink, T. A., and Raines, R. T. (2000) Conformational stability is a determinant of ribonuclease A cytotoxicity, *J. Biol. Chem. 275*, 17463−17467.
27. Dickson, K. A., Dahlberg, C. L., and Raines, R. T. (2003) Compensating effects on the cytotoxicity of ribonuclease A variants, *Arch. Biochem. Biophys. 415*, 172−177.
28. Raines, R. T. (1998) Ribonuclease A, *Chem. Rev. 98*, 1045−1065.
29. Futami, J., Maeda, T., Kitazoe, M., Nukui, E., Tada, H., Seno, M., Kosaka, M., and Yamada, H. (2001) Preparation of potent cytotoxic ribonucleases by cationization: Enhanced cellular uptake and decreased interaction with ribonuclease inhibitor by chemical modification of carboxyl groups, *Biochemistry 26*, 7518−7524.
30. Futami, J., Nukui, K., Maeda, T., Kosaka, M., Tada, H., Seno, M., and Yamada, H. (2002) Optimum modification for the highest cytotoxicity of cationized ribonuclease, *J. Biochem. (Tokyo) 132*, 223−228.
31. Ilinskaya, O. N., Dreyer, F., Mitkevich, V. A., Shaw, K. L., Pace, C. N., and Makarov, A. A. (2002) Changing the net charge from negative to positive makes ribonuclease Sa cytotoxic, *Protein Sci. 11*, 2522−2525.
32. Ilinskaya, O. N., Koschinski, A., Mitkevich, V. A., Repp, H., Dreyer, F., Pace, C. N., and Makarov, A. A. (2004) Cytotoxicity of RNases is increased by cationization and counteracted by K(Ca) channels, *Biochem. Biophys. Res. Commun. 314*, 550−554.
33. Fuchs, S. M., Rutkoski, T. J., Kung, V. M., Groeschl, R. T., and Raines, R. T. (2007) Increasing the cytotoxicity of ribonuclease A with arginine grafting, *Protein Eng., Des. Sel.*, in press.
34. Ogawa, Y., Iwama, M., Ohgi, K., Tsuji, T., Irie, M., Itagaki, T., Kobayashi, H., and Inokuchi, N. (2002) Effect of replacing the aspartic acid/glutamic acid residues of bullfrog sialic acid binding lectin with asparagine/glutamine and arginine on the inhibition of cell proliferation in murine leukemia P388 cells, *Biol. Pharm. Bull. 25*, 722−727.
35. Chandran, S. S., Dickson, K. A., and Raines, R. T. (2005) Latent fluorophore based on the trimethyl lock, *J. Am. Chem. Soc. 127*, 1652−1653.
36. Lavis, L. D., Chao, T.-Y., and Raines, R. T. (2006) Fluorogenic label for biomolecular imaging, *ACS Chem. Biol. 1*, 252−260.
37. Smith, B. D., Soellner, M. B., and Raines, R. T. (2003) Potent inhibition of ribonuclease A by oligo(vinylsulfonic acid), *J. Biol. Chem. 278*, 20934−20938.
38. Leland, P. A., Staniszewski, K. E., Kim, B.-M., and Raines, R. T. (2001) Endowing human pancreatic ribonuclease with toxicity for cancer cells, *J. Biol. Chem. 276*, 43095−43102.
39. Rutkoski, T. J., Kurten, E. L., Mitchell, J. C., and Raines, R. T. (2005) Disruption of shape-complentarity markers to create cytotoxic variants of ribonuclease A, *J. Mol. Biol. 354*, 41−54.
40. Johnson, R. J., McCoy, J. G., Bingman, C. A., Phillips, G. N., Jr., and Raines, R. T. (2007) Inhibition of human pancreatic ribonuclease by the human ribonuclease inhibitor protein, *J. Mol. Biol. 368*, 434−449.
41. Riddles, P. W., Blakeley, R. L., and Zerner, B. (1983) Reassessment of Ellman's reagent, *Methods Enzymol. 91*, 49−60.
42. Kelemen, B. R., Klink, T. A., Behlke, M. A., Eubanks, S. R., Leland, P. A., and Raines, R. T. (1999) Hypersensitive substrate for ribonucleases, *Nucleic Acids Res. 27*, 3696−3701.
43. Abel, R. L., Haigis, M. C., Park, C., and Raines, R. T. (2002) Fluorescence assay for the binding of ribonuclease A to the ribonuclease inhibitor protein, *Anal. Biochem. 306*, 100−107.
44. Haigis, M. C., Kurten, E. L., Abel, R. L., and Raines, R. T. (2002) KFERQ sequence in ribonuclease A-mediated cytotoxicity, *J. Biol. Chem. 277*, 11576−11581.
45. Bosch, M., Benito, A., Ribó, M., Puig, T., Beaumelle, B., and Vilanova, M. (2004) A nuclear localization sequence endows human pancreatic ribonuclease with cytotoxic activity, *Biochemistry 43*, 2167−2177.
46. Kim, J.-S., Souček, J., Matoušek, J., and Raines, R. T. (1995) Catalytic activity of bovine seminal ribonuclease is essential for its immunosuppressive and other biological activities, *Biochem. J. 308*, 547−550.
47. Leland, P. A., Schultz, L. W., Kim, B.-M., and Raines, R. T. (1998) Ribonuclease A variants with potent cytotoxic activity, *Proc. Natl. Acad. Sci. U.S.A. 98*, 10407−10412.
48. Fuchs, S. M., and Raines, R. T. (2007) Arginine grafting to endow cell permeability, *ACS Chem. Biol. 2*, 167−170.
49. Saxena, S. K., Rybak, S. M., Winkler, G., Meade, H. M., McGray, P., Youle, R. J., and Ackerman, E. J. (1991) Comparison of RNases and toxins upon injection into *Xenopus* oocytes, *J. Biol. Chem. 266*, 21208−21214.
50. Hallbrink, M., Floren, A., Elmquist, A., Pooga, M., Bartfai, T., and Langel, U. (2001) Cargo delivery kinetics of cell-penetrating peptides, *Biochim. Biophys. Acta 1515*, 101−109.
51. Soncin, F., Strydom, D. J., and Shapiro, R. (1997) Interaction of heparin with human angiogenin, *J. Biol. Chem. 272*, 9818−9824.

52. Slivinsky, G. G., Hymer, W. C., Bauer, J., and Morrison, D. R. (1997) Cellular electrophoretic mobility data: A first approach to a database, *Electrophoresis 18*, 1109−1119.
53. Orntoft, T. F., and Vestergaard, E. M. (1999) Clinical aspects of altered glycosylation of glycoproteins in cancer, *Electrophoresis 20*, 362−371.
54. Haigis, M. C., Kurten, E. L., and Raines, R. T. (2003) Ribonuclease inhibitor as an intracellular sentry, *Nucleic Acids Res. 31*, 1024−1032.

BI700857U